INPC 2025

NucleiML

A machine learning tool for finite nuclei properties

Sarmistha Banik

BITS Pilani Hyderabad Campus

Introduction

Equation of State

- ρ_0
- E_0
- K_0
- Q_0
- J_0
- L_0
- m^*/m

$\rightarrow$

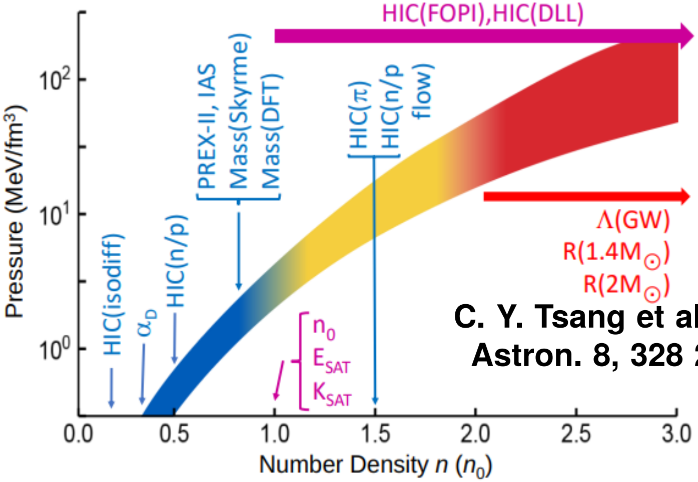

C. Y. Tsang et al, Nat. Astron. 8, 328 2024

Constraints at High densities

- Constraints from GW and NICER observations
- GW[1] : GW170817 BNS merger
- NICER[2] : simultaneous mass-radius measurements

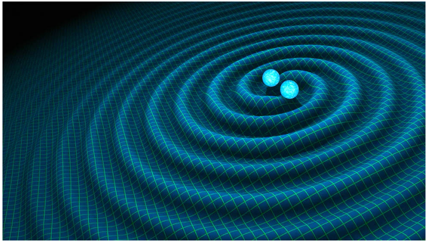

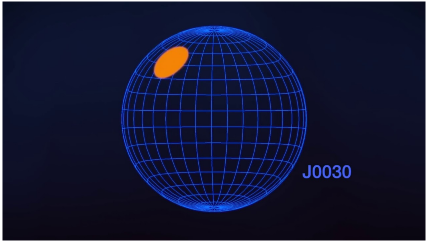

[1] Image from **R. Hurt/Caltech-JPL**
[2] Image from **NICER (NASA)**

Constraints at low densities

- Constraints from Heavy Ion Collisions[3] (HICs) and Nuclear physics experiments
- HICs : on symmetry energy and pressure across different densities [4]
- Nuclear Physics : Constraints on global behavior of EoS when included explicitly [5]

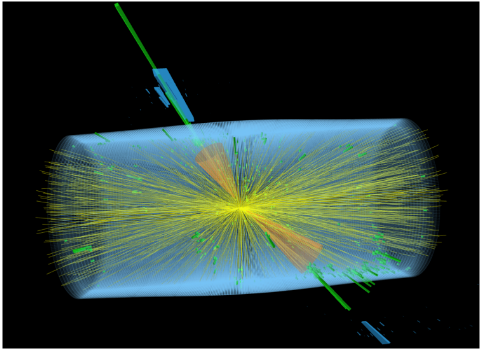

[3] Representative image from CMS collaboration
[4] C. Y. Tsang et al, Nat. Astron. 8, 328 2024
[5] **A. Venneti et al 2024, PLB 854, 138756**

Constraints at low densities

- Constraints from Heavy Ion Collisions (HICs) and Nuclear physics experiments
- HICs : on symmetry energy and pressure across different densities [6]
- Nuclear Physics : Constraints on global behavior of EoS when included explicitly [7]

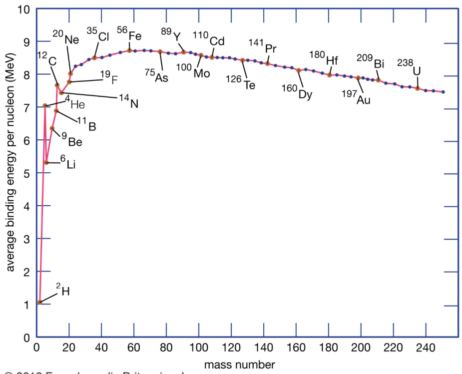

[6] C. Y. Tsang et al, Nat. Astron. 8, 328 2024

[7] **A. Venneti et al 2024, PLB 854, 138756**

Implicit and Explicit constraints

Implicit Constraints[8]

- Constraints from HICs and Nuclear physics experiments through limits on symmetry energy $J(\rho)$ and $P(\rho)$ at different densities as well as through NS properties
- Includes those from analyses of nuclear masses

Explicit Constraints[9]

- Constraints similar to Implicit
- Instead of implicit constraints of nuclear masses, we used explicit constraints on binding energies and charge radii of different nuclei

---

[8] C. Y. Tsang et al, Nat. Astron. 8, 328 2024

[9] **A. Venneti et al 2024, PLB 854, 138756**

Implicit and Explicit constraints

Key points

- Different approaches to include low density nuclear physics constraints have distinct posterior distributions of the parameters
- Highlights the importance of explicitly constraining finite nuclei properties
- However, computational cost is challenging to extend these explicit constraints to a large diverse set of nuclei
- Present work of NucleiML framework addresses this challenge, with help of machine learning

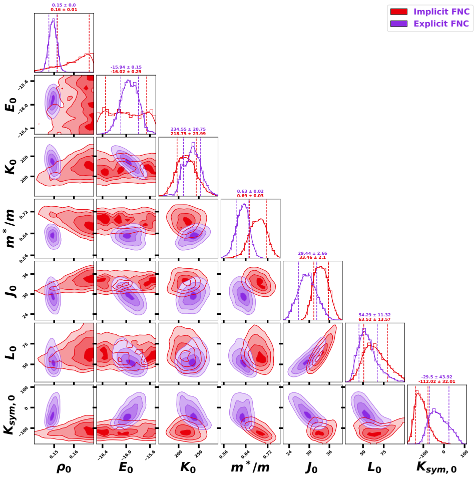

Formalism

$$\mathcal{L}_{NL} = \mathcal{L}_{nm} + \mathcal{L}_{\sigma} + \mathcal{L}_{\omega} + \mathcal{L}_{\rho} + \mathcal{L}_{int},$$

- $\mathcal{L}_{nm}$: Nucleons[10]: protons and neutrons
- $\mathcal{L}_{\sigma}$: σ-meson : short range attraction
- $\mathcal{L}_{\omega}$: ω-meson : very short range repulsion
- $\mathcal{L}_{\rho}$: ρ-meson : isospin dependent

[10] **M Dutra et al., Phys. Rev. C 90, 055203 2014.**

Interaction strength determined by coupling parameters : g_σ, g_ω, g_ρ, A, B, C, and Λ_v

$$
\begin{aligned}
\mathcal{L}_{nm} &= \bar{\psi}\left(i\gamma^\mu\partial_\mu - m\right)\psi + g_\sigma\sigma\bar{\psi}\psi - g_\omega\bar{\psi}\gamma^\mu\omega_\mu\psi \\
&\quad -\frac{g_\rho}{2}\bar{\psi}\gamma^\mu\vec{\rho}_\mu\vec{\tau}\psi, \\
\mathcal{L}_\sigma &= \frac{1}{2}\left(\partial^\mu\sigma\partial_\mu\sigma - m_\sigma^2\sigma^2\right) - \frac{A}{3}\sigma^3 - \frac{B}{4}\sigma^4, \\
\mathcal{L}_\omega &= -\frac{1}{4}\Omega^{\mu\nu}\Omega_{\mu\nu} + \frac{1}{2}m_\omega^2\omega^\mu\omega_\mu + \frac{C}{4}\left(g_\omega^2\omega_\mu\omega^\mu\right)^2, \\
\mathcal{L}_\rho &= -\frac{1}{4}\vec{B}^{\mu\nu}\vec{B}_{\mu\nu} + \frac{1}{2}m_\rho^2\vec{\rho}_\mu\vec{\rho}^\mu, \\
\mathcal{L}_{int} &= \frac{1}{2}\Lambda_v g_\omega^2 g_\rho^2\omega_\mu\omega^\mu\vec{\rho}_\mu\vec{\rho}^\mu.
\end{aligned}
$$

Algorithm of RMF

NMPs

↓

$g_\sigma,\ g_\omega,\ g_\rho,\ A,\ B,\ C,\ \Lambda_v$

↓

Solving the field equations

Gambhir et al, Ann. Phys. 198, 132 1990

$$g_\sigma,\ g_\omega,\ g_\rho,\ A,\ B,\ C,\ \Lambda_v$$

Solving the field equations
using basis expansion

Gambhir et al, Ann. Phys. 198, 132 1990

Algorithm of RMF

↓

Solving the Field equations
Using basis expansion

↓

calculating binding energy and
charge radius of given nuclei $^{A}\mathrm{X}_{Z}$

Gambhir et al, Ann. Phys. 198, 132 1990

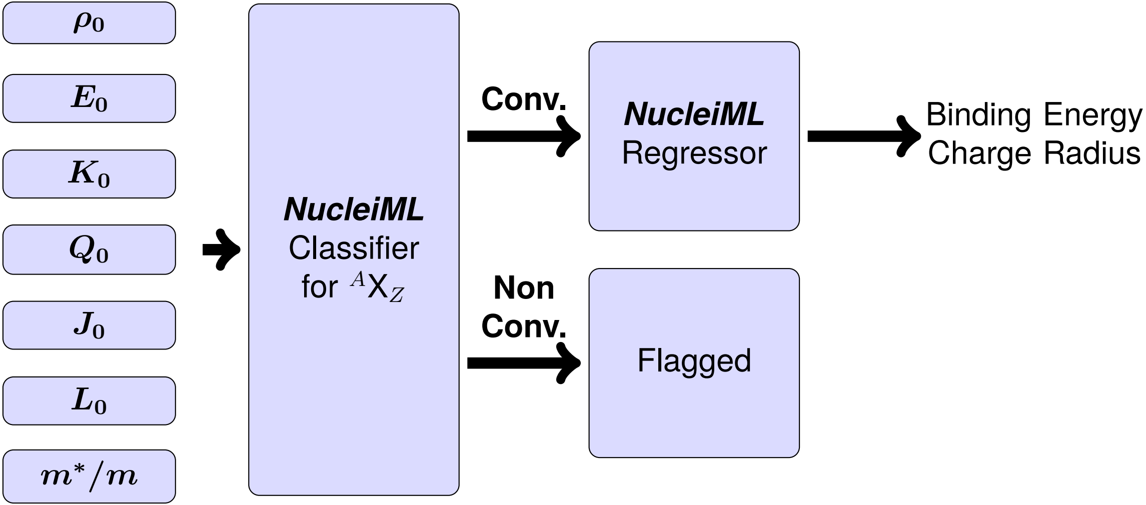

ρ_0
E_0
K_0
Q_0
J_0
L_0
m^*/m
NucleiML
Classifier
for ^{A}X$_Z$
Conv.
Non
Conv.
NucleiML
Regressor
Flagged
Binding Energy
Charge Radius

Neural Network Training and Performance

Classifier

- **Dataset Construction**: Randomly sampled seven NMPs determine the coupling constants
- **Data Composition:** Each data point includes NMPs, coupling parameters, BE, R_{ch} and a classification flag (*Convergent*, *Non-convergent A/B/C*).
- **Classifier Training:** The model is trained using categorical cross-entropy, with performance validated on a separate set to ensure generalization.
- **Performance:** Training stabilizes with 0.2 loss and 92% accuracy, showing effective learning and minimal overfitting.

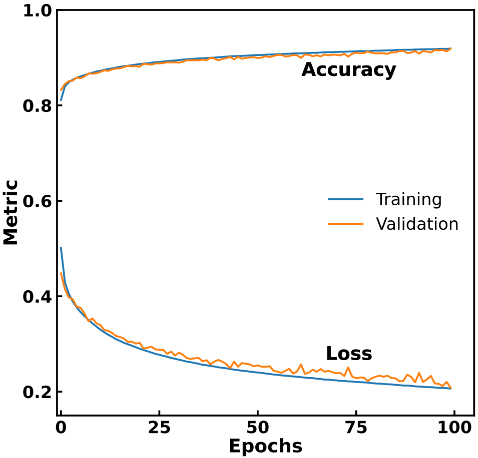

Classifier

- **Confusion Matrix:** true vs. predicted labels; diagonals indicate correct classifications, off-diagonals show misclassifications.
- **Classifier Strengths:** Strong classification accuracy for *Convergent* and *Non-convergent B*, with decent performance on *Non-convergent A*.
- **Class Imbalance Impact:** Low accuracy for *Non-convergent C* is due to its low representation in the training data.
- **Four-Class Justification:** Maintaining four classes enhances distinction from *Convergent* cases, supporting better performance in Bayesian inference by reducing misclassification and improving sampling reliability.

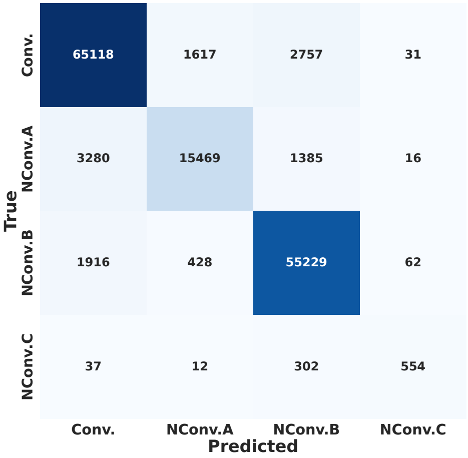

Regressor

- **Deviation Metric:** Prediction accuracy is assessed using relative deviation, $\frac{\Delta X}{X} = \frac{X_{true} - X_{pred}}{X_{true}}$, where X is BE or charge radius.
- **Distribution Analysis:** deviation distributions peaking near zero, indicating high prediction accuracy.
- **Confidence Intervals:** 95% of BE predictions fall within 3–5% deviation; for charge radius, within 1%.
- **Regressor Precision:** Tighter CI and narrower distribution for charge radius highlight superior prediction performance.
- **Reasoning:** Higher accuracy for charge radius is due to its more constrained range across nuclei compared to BE.

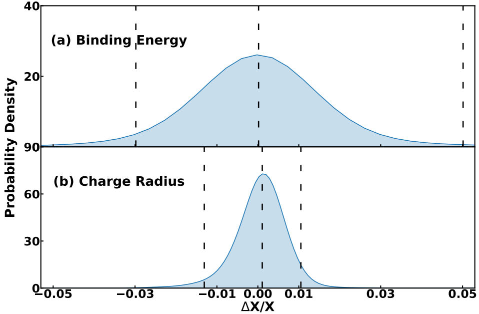

Performance

- **Initial Limitation:** The original regressor, trained on five closed-shell nuclei, shows broad deviations when predicting unseen nuclei, indicating poor generalization.
- **Training Set Expansion:** Adding neutron-rich nuclei (^{24}O, ^{58}Ca, ^{78}Ni) improves prediction accuracy, with a narrower deviation distribution and median closer to zero.
- **Further Refinement:** Including ^{68}Ni and ^{90}Zr further reduces deviation spread, confirming that a diverse training set enhances regressor performance on untrained nuclei.

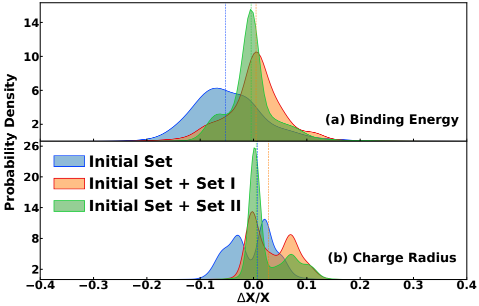

Binding energy of some Nuclei

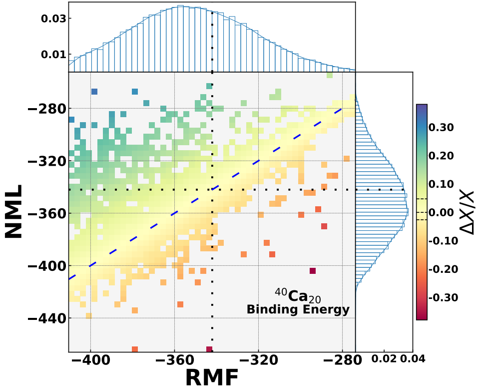

The NML regressor closely replicates RMF predictions for nuclei like ^{40}Ca and ^{208}Pb, with deviations mostly within ±5% for BE and ±1% for R$_{ch}$.

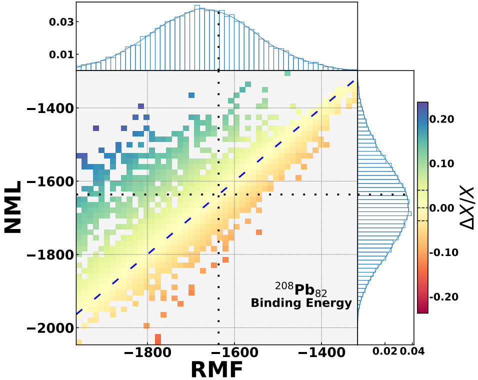

This indicates that the model closely approximates RMF results, with slightly greater variability in binding energy predictions compared to charge radius estimates.

A Bayesian Example

Bayesian Run

- **Implmentation in a bayesian analysis** - An effective way to analyze the accuracy of NucleiML model
- Posteriors of *NucleiML* align well with those of RMF model
- NML enables 10× faster Bayesian inference than RMF (30 min vs. 4.5 hrs) with comparable posterior distributions.

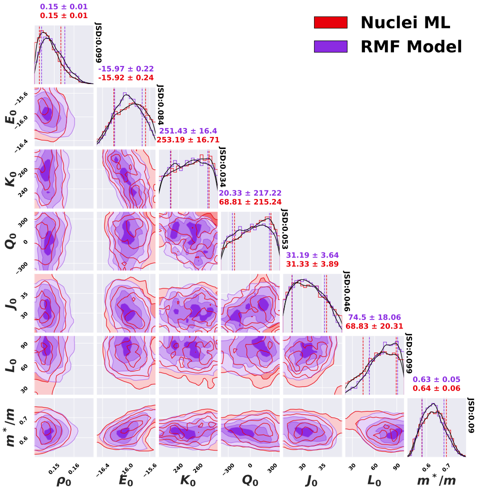

Conclusion and future outlook

Key takeaways

- **NML Framework**: NucleiML (NML) uses a Classifier and two Regressors to replicate RMF predictions for binding energies and charge radii.
- **Model Accuracy**: The Classifier achieves 92% accuracy; Regressors predict nuclear properties within 5% error for 95% of the test set.
- **Generalization:** Accuracy improves on unseen nuclei when trained on a more diverse dataset.
- **Bayesian Integration:** NML enables 10× faster Bayesian inference than RMF (30 min vs. 4.5 hrs) with comparable posterior distributions.

Thank you

Birla Institute of Technology and Sciences, Pilani
Hyderabad Campus

Work Presented here is from
"NucleiML: A machine learning framework of ground-state properties of finite nuclei for accelerated Bayesian exploration"
Venneti A, Mondal C, Imam SMA, **Banik S**, and Agrawal BK
In Review, arXiv:2504.03333

Do we need hadron-quark phase transitions inside neutron star cores to satisfy nuclear and astrophysical observations?

Bayesian with hadronic and hybrid EOSs*

- hybrid EOS model = Crust + Relativistic Mean Field model [Malik et al., Phys. Rev. D (2023)] + phase transition [Albino et al., J. Phys.: Conf. Series (2022)] + **Mean Field theory of Quantum Chromodynamics** [Fogaça et al., Phys. Lett. B (2011)]
- Bayesian analysis with constraints from PSR J0030+0451, PSR J0740+6620, and PSR J0437-4715 and GW170817
- smooth hybrid EOSs are slightly more favoured according to pulsar observations but GW data remains indecisive

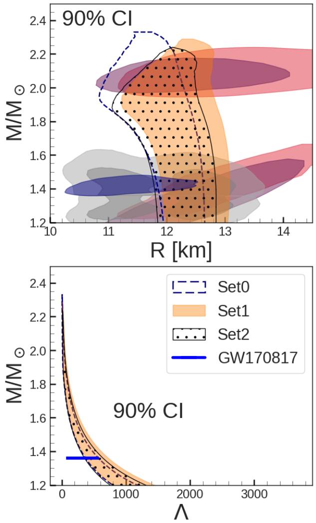

---

* **Bayesian evaluation of hadron-quark phase transition models through neutron star observables in light of nuclear and astrophysics data**
D. Guha Roy, A. Venneti, T. Malik, S. Bhattacharya, **S. Banik**
Phys. Lett. B 859 (2024) 139128

Conformality of matter inside hybrid stars

- parameter $d_c = \sqrt{\Delta^2 + (\Delta')^2}$, where Δ is renormalized trace anomaly, proposed in Annala et al., Nature Commun. (2023), as a measure of conformality
- quark matter remains strongly interacting, and the conformal limit is not reached at the NS center
- even with purely nucleonic degrees of freedom, d_c gradually decreases below 0.2 around 5 $\rho_{B,0}$
- for hybrid models d_c crosses this threshold at lower densities
- threshold value for d_c (horizontal dashed line) might not be universally applicable across models